Selective control of molecule charge state on graphene using tip-induced electric field and nitrogen doping

van Dong Pham, Sukanya Ghosh, Frédéric Joucken, Mario Pelaez-Fernandez, Vincent Repain, Cyril Chacon, Amandine Bellec, Yann Girard, Robert Sporken, Sylvie Rousset, et al.

npj | 2D Materials and Applications

www.nature.com/npj2dmaterials

ARTICLE OPEN

Selective control of molecule charge state on graphene using tip-induced electric field and nitrogen doping

Van Dong Pham[1,5], Sukanya Ghosh[2,6], Frédéric Joucken[3], Mario Pelaez-Fernandez[1,7], Vincent Repain[1], Cyril Chacon[1], Amandine Bellec[1], Yann Girard[1], Robert Sporken[3], Sylvie Rousset[1], Yannick J. Dappe[4], Shobhana Narasimhan[2] and Jérôme Lagoute[1]

The combination of graphene with molecules offers promising opportunities to achieve new functionalities. In these hybrid structures, interfacial charge transfer plays a key role in the electronic properties and thus has to be understood and mastered. Using scanning tunneling microscopy and ab initio density functional theory calculations, we show that combining nitrogen doping of graphene with an electric field allows for a selective control of the charge state in a molecular layer on graphene. On pristine graphene, the local gating applied by the tip induces a shift of the molecular levels of adsorbed molecules and can be used to control their charge state. Ab initio calculations show that under the application of an electric field, the hybrid molecule/graphene system behaves like an electrostatic dipole with opposite charges in the molecule and graphene sub-units that are found to be proportional to the electric field amplitude, which thereby controls the charge transfer. When local gating is combined with nitrogen doping of graphene, the charging voltage of molecules on nitrogen is greatly lowered. Consequently, applying the proper electric field allows one to obtain a molecular layer with a mixed charge state, where a selective reduction is performed on single molecules at nitrogen sites.

npj 2D Materials and Applications (2019)3:5 ; https://doi.org/10.1038/s41699-019-0087-5

INTRODUCTION

The interface between organic molecules and graphene is the focus of growing interest for combined molecular and graphene-based electronics.[1] Interfacial charge transfer is a key factor that controls the interface dipole, electronic doping, and chemical acitivity. Using electron donor or acceptor molecules, it is possible to achieve n-type or p-type doping of graphene by non-covalent functionalization.[2–7] However, the nature of the molecules is not the only parameter determining the charge transfer. Applying an external electric field or using functionalized graphene also allows one to tailor the electronic interaction of molecules with graphene. Recent scanning tunneling microscopy (STM) experiments have shown that a gate voltage can tune the charge state of a molecule on graphene and the alignment of the molecular states.[8,9] The molecule/graphene interface can also be tuned using chemically doped graphene, whereby foreign atoms are subsituted for carbon atoms. Among the possible doping elements, the case of nitrogen has been widely investigated,[10–13] since it allows one to perform n-doping without inducing structural relaxations, while preserving the Dirac cone in the band structure. It has been shown that nitrogen doping improves the performance of graphene devices such as sensors or capacitors, due to local variations in chemical reactivity or charge transfer at the doping sites.[14,15] It is therefore necessary to understand the electronic interaction of graphene with molecules at the single molecule level. Recently, STM experiments have shown that molecules adsorbed at nitrogen sites exhibit a different electronic spectrum from those adsorbed on pristine areas, with a shifted or reduced electronic gap.[16–18] The effect of an applied electric field on these hybrid systems has however not yet been studied.

Here, we study the effect of tip-induced electric fields in STM experiments on the charge state of molecules on both pristine and nitrogen-doped graphene. We show that the tip-induced electric field shifts the molecular levels, allowing one to change the charge state of the molecules. Combining this electric field effect with chemical doping of graphene allows one to achieve a selective reduction of a single molecule in a monolayer of organic molecules on the surface of graphene. We use STM and ab initio density functional theory (DFT) calculations to study a model system comprising tetracyanoquinodimethane (TCNQ) molecules on multilayer graphene on a SiC(000$\bar{1}$) substrate. TCNQ is a well-known electron acceptor, that has previously been investigated by STM on a variety of substrates.[19–22]

RESULTS AND DISCUSSION

Figure 1a shows a STM image of a TCNQ molecular island self-assembled on pristine graphene, exhibiting a nearly square lattice with unit cell vectors of lengths $a = 0.93 \pm 0.01$ nm, $b = 0.89 \pm 0.02$ nm, and angle $\theta = 85 \pm 2°$ [Fig. 1b]. The structure of the molecular layer is well reproduced by the calculations [see Fig. S1 in Supplementary Information].

[1]Université Paris Diderot, Sorbonne Paris Cité, CNRS, Laboratoire Matériaux et Phénomènes Quantiques, UMR 7162, 75013 Paris, France; [2]Theoretical Sciences Unit and School of Advanced Materials, Jawaharlal Nehru Centre for Advanced Scientific Research, Jakkur, Bangalore 560064, India; [3]Research Center in Physics of Matter and Radiation (PMR), University of Namur (FUNDP), 61 Rue de Bruxelles, 5000 Namur, Belgium and [4]SPEC, CEA, CNRS, Université Paris-Saclay, CEA Saclay, 91191 Gif-sur-Yvette Cedex, France
Correspondence: Jérôme. Lagoute (jerome.lagoute@univ-paris-diderot.fr)
[5]Present address: Paul-Drude-Institut für Festkörperelektronik, Hausvogteiplatz 5-7, 10117 Berlin, Germany
[6]Present address: Abdus Salam International Centre for Theoretical Physics, Strada Costiera 11, Trieste I-34151, Italy
[7]Present address: Laboratorio de Microscopias Avanzadas (LMA), Instituto de Nanociencia de Aragon (INA), Universidad de Zaragoza, Zaragoza, Spain

Received: 9 August 2018 Accepted: 27 December 2018
Published online: 25 January 2019

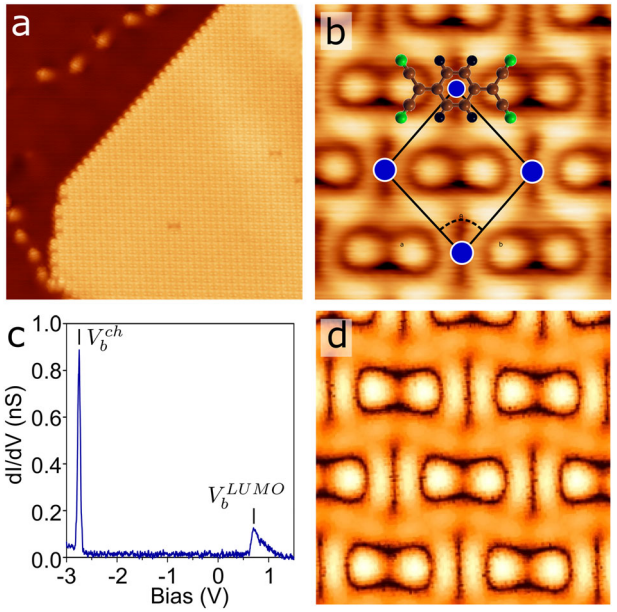

Fig. 1 2D island of TCNQ molecules on pristine graphene. **a** Large-scale STM image (30×30 nm^2, $V = 1$ V, $I = 30$ pA). **b** Zoomed-in STM image (2.5×2.5 nm^2, $V = 1$ V, $I = 30$ pA) with superimposed unit cell and atomic structure of the TCNQ molecule (H—black, C—brown, N—green). **c** Representative d*I*/d*V* spectrum recorded above a TCNQ molecule. **d** Simulated STM image at the calculated LUMO energy (0.12 V) of the TCNQ molecular layer on monolayer graphene

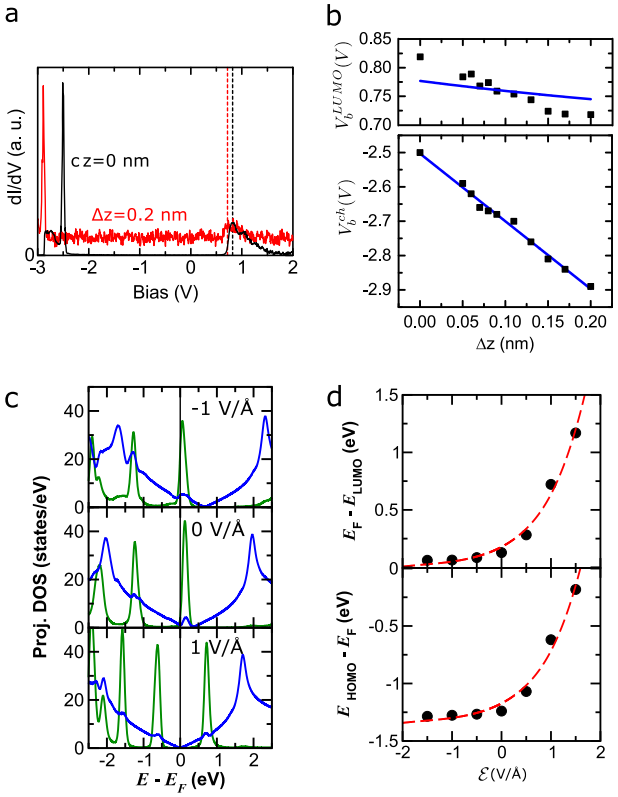

Fig. 2 Effect of varying electric field on spectra of TCNQ on pristine graphene. **a** d*I*/d*V* spectra measured (−1.5 V, 15 pA) on a TCNQ molecule when the tip is at the setpoint position ($\Delta z = 0$ nm), and when it is retracted from it by 0.2 nm ($\Delta z = 0.2$ nm). **b** Positions of the charging peak and of the LUMO peak as a function of the tip-sample vertical retraction [same molecule and setpoint as in **a**]. The blue lines are fits to the model described in the text. **c** Projected density of states, from DFT, on the graphene atoms (blue curve) and molecule (green curve) at three values of applied electric field. **d** Results from DFT for change in the position of the HOMO and LUMO states of TCNQ/graphene as a function of the applied electric field; dashed lines are a guide to the eye

Differential conductance (d*I*/d*V*) spectroscopy on TCNQ exhibits a broad resonance at positive bias, and a sharp peak at negative bias [Fig. 1c]. The experimental STM image in Fig. 1b, recorded at a bias voltage of 1 V, is fairly well reproduced by the simulated STM image calculated from DFT at a bias corresponding to the energy of the lowest unoccupied molecular orbital (LUMO) state for the TCNQ on graphene system [Fig. 1d]; it is also similar to that reported previously for the LUMO state of self-organized TCNQ on graphene on Ir(111).[20,21] The peak around the bias voltage $V_b^{\mathrm{LUMO}} = 0.75\,\mathrm{V} \pm 0.05\,\mathrm{V}$ is therefore attributed to arise from the LUMO state of the TCNQ molecules. It has to be noted that this peak appears asymmetric with a shoulder on the right side. We attribute this to the presence of a satellite peak above the LUMO peak. This can be seen more clearly in Fig. 2a (black curve). Such satellite peaks have been reported for F_4TCNQ adsorbed on graphene on hBN[9] and attributed to vibronic transitions. In the spectrum reported in Fig. 2a we measure an energy separation between the LUMO peak and the satellite peak of 0.22 V, which is very close to the value measured on F_4TCNQ.[9] Therefore, we attribute the asymmetry of the LUMO peak to the presence of vibronic peaks.

The sharp peak at a negative bias V_b^{ch} has a different physical origin. It shifts significantly upon changing the tip-sample distance *z*, as shown in Fig. 2a, b. Remarkably, the peak (at positive bias) corresponding to the LUMO state also exhibits a shift with *z* (see Fig. 2b and Fig. S2 in Supplementary Information), which is not at all expected for a molecular resonance when a molecule is in direct contact with a conductive surface; the origin of this shift will be explained further below. Spectroscopic features similar to these sharp peaks at negative bias have previously been observed for other adsorbates on various surfaces.[23–28] Their origin has been attributed to a charging of the adsorbate induced by the electric field of the tip, that shifts an adsorbate state to the Fermi level through a band bending effect. Thus, the sharp peak at negative bias arises from a charging of the molecule and not from the HOMO state.

To verify whether the position of the LUMO state is indeed influenced by the application of an electric field, we next examine changes in the projected density of states (PDOS) of the molecule and graphene, as calculated from DFT, upon varying the strength of an applied vertical electric field. Examples of the PDOS at three values of electric field are shown in Fig. 2c (note that the position of the LUMO is shifted in the calculations with respect to the experiment, this is a well-known shortcoming of DFT). Our results show that the highest occupied molecular orbital (HOMO) and LUMO peaks are downshifted when a negative (from molecule to graphene) electric field is applied, while they shift in the opposite direction for a positive electric field [note the displacement of the green peaks in Fig. 2c]. Remarkably, Fig. 2c also shows that, at the same time, the graphene PDOS shifts in the opposite direction (note the displacement of the blue curves in the graphs). As will be shown below, this arises from an electric field-dependent charge transfer between graphene and the TCNQ molecules. These shifts are also clearly visible in Fig. 2d, where we have plotted how the calculated HOMO and LUMO energies vary with the applied electric field. Note that when the LUMO state is separated from the Fermi level, E_{LUMO} varies almost linearly with the electric field with a slope of 0.9 nm. This behavior is quite different from the expectation that an electric field would change the chemical potential of the sample surface, leading to a rigid shift in the spectrum of the entire molecules + graphene system.

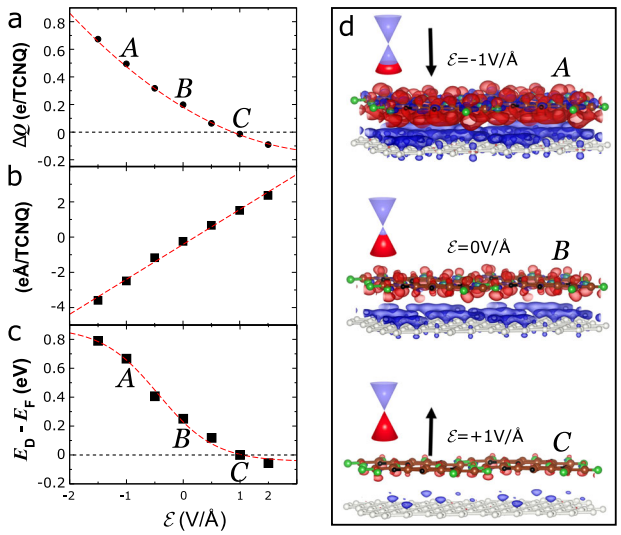

Fig. 3 Results from DFT calculations on TCNQ/graphene under a vertical external electric field $\mathcal{E}$. **a** Charge gained by TCNQ molecule (ΔQ_{TCNQ}) as a function of $\mathcal{E}$. **b** Dipole moment μ of the TCNQ/graphene system. **c** Energy of the Dirac point with respect to the Fermi level as a function of $\mathcal{E}$. **d** Isosurfaces (0.0007 e/bohr^3) of the charge density difference $\Delta\rho$ for three values of the electric field. Red/blue lobes correspond to electron accumulation/depletion, respectively. Color code for atoms: C (of graphene)—gray, C (of TCNQ)—brown, H—black, N—green. Color code for Dirac cone schemes: blue—empty states, red—filled states

Our results show that, on the contrary, the molecular states are not pinned to the Dirac point, under an electric field. It is important to note that our calculations do not include the field effect that occurs in gated devices, since there is no closed connection that would allow a charge flow with a gate. The calculated shifts thus correspond to the shift induced by a variation of molecule-graphene charge transfer. In a gated device geometry, this effect should be added to the variation of the chemical potential of the graphene due to the gate field. We also emphasize that one implication of the electric field effect is that the LUMO peak observed experimentally is shifted due to the tip-sample electric field, meaning that the measured energy of the molecular state is shifted to higher energies, and thus values extracted from scanning tunneling spectroscopy (STS) need to be corrected.

To quantify the shift of the LUMO state, we consider a linear dependence of the LUMO state U_0 with the electric field $\mathcal{E}$. This is expected when the density of states of the molecule is constant around the Fermi level (which occurs when the HOMO and LUMO states are well separated from the Fermi level) and the molecule/graphene system behaves as an induced dipole (see the discussion below). In such a case, the charge of the molecule is proportional to the electric field, and the molecular spectrum will shift proportionally to the electric field. When a negative bias is applied, the LUMO state shifts to $U_0 + \kappa\mathcal{E}$ where κ is the proportionality factor relating the energy shift to the electric field. The charging process occurs when the LUMO state is at the Fermi energy i.e., when $U_0 + \kappa\mathcal{E} = 0$. Assuming a planar junction geometry, the electric field can be written as $\mathcal{E} = V_b/(z_0 + \Delta z)$, where V_b is the bias voltage applied, z_0 is the tip-sample separation at the setpoint position, and Δz is the tip-sample separation difference with respect to z_0. The charging peak appears when $V_b^{ch} = -U_0 z_0/\kappa - U_0\Delta z/\kappa$. The energy position of this peak therefore depends linearly on the tip-sample separation, as also observed experimentally [see Fig. 2b, lower panel]. A linear fit to the experimental data gives $U_0/\kappa = 1.97$ V/nm and $z_0 = 1.3$ nm. For the LUMO state, the peak appears when $V_b^{LUMO} = (z_0 + \Delta z)U_0/(z_0 + \Delta z - \kappa)$. The best agreement with the experimental data are obtained for $U_0 = 0.6$ V [blue curve in Fig. 2b] leading to $\kappa = 0.3$ nm which is in the same range as the slope of 0.9 nm mentioned above in the DFT calculation. This suggests that in the experiments, the position of the LUMO is overestimated by about 150 mV. Note that our model [see the blue curves in Fig. 2b] correctly predicts that varying the tip height has a large impact on the measured position of the charging peak, but a much smaller impact on the position of the LUMO peak. It should also be noted that in the limit of $\kappa/z_0 \ll 1$, the present model leads to equations of the same form as a dual capacitance model (see supplementary information). However, only the former model incorporates the charge transfer between the molecule and the substrate that comes out from the *ab initio* calculations.

To gain further insight into the physical origin of the electric field effect on TCNQ/graphene, we examine our results from DFT, for how the charge transfer between graphene and TCNQ is affected by the application of the electric field [Fig. 3a]. We see that the charge ΔQ gained by TCNQ from graphene varies monotonically with the electric field. A negative electric field induces an increased accumulation of electrons in TCNQ and a depletion in graphene, whereas a positive electric field reverses this tendency. Interestingly, we see that at a sufficiently large-positive electric field higher than 1 V/Å, the direction of charge transfer can be reversed, even though TCNQ is known to be an electron acceptor. In Fig. 3b the computed electric dipole moment μ of the molecule on graphene system is reported. The nearly linear variation of μ with $\mathcal{E}$ indicates that the TCNQ/graphene structure behaves like an induced electrostatic dipole. From the slope of Fig. 3b we find the vertical (perpendicular to the graphene plane) polarizability α of the TCNQ/graphene system to be 29 Å^3/molecule. This value is larger than the polarizability of a single TCNQ molecule in the gas phase, that we find to be 12.9 Å^3/molecule in the direction perpendicular to the molecular plane, in good agreement with previous studies.[29,30] The larger polarizability of the hybrid structure is attributed to its larger extension along the vertical direction with respect to a single molecule.

A consequence of the electric field-driven charge transfer is that the position of the Dirac point of graphene changes upon the application of an electric field, in accordance with the charge exchange with the molecule; this variation is plotted in Fig. 3c. Alongside, we show, in Fig. 3d, the evolution of the spatial redistribution of electron density; here we have plotted isosurfaces of $\Delta\rho = \rho^{\text{TCNQ/graphene}} - \rho^{\text{TCNQ}} - \rho^{\text{graphene}}$, where ρ^X is the electronic charge density for the system X. We see that at zero electric field (image *B*), electrons are transferred from graphene to the molecules, which is to be expected, since TCNQ is known to be an electron acceptor. We also see that at negative electric field (image *A*) this charge redistribution is reinforced, whereas it is reduced at positive electric field (image *C*).

Finally, we combine the electric field-induced charge transfer with nitrogen doping of graphene in order to achieve a selective reduction of a single TCNQ molecule in a 2D molecular lattice. On nitrogen (N) doped graphene, it has been shown that when a molecule is adsorbed above a N-site, the molecular states' energies are downshifted due to a local charge transfer.[16] Therefore the charging energy of a molecule above a N-site is expected to be different from that of the surrounding molecules above carbon sites (C-sites). In Fig. 4a we show a TCNQ molecular island on N-doped graphene. The molecule adsorbed above a N-site appears brighter. This contrast is due to an electronic effect since it depends on the imaging bias voltage [at +1 V all the molecules appear identical (Fig. 4b) while a contrast is observed at −1.5 V (Fig. 4c)].

The local charge transfer at the N-site is revealed by a shift of the LUMO state from 0.8 ± 0.06 V on C-sites to 0.35 ± 0.06 V on N-sites [Fig. 4e]. This shift reveals a larger charge transfer from graphene to TCNQ molecules at N-sites, similar to what has been

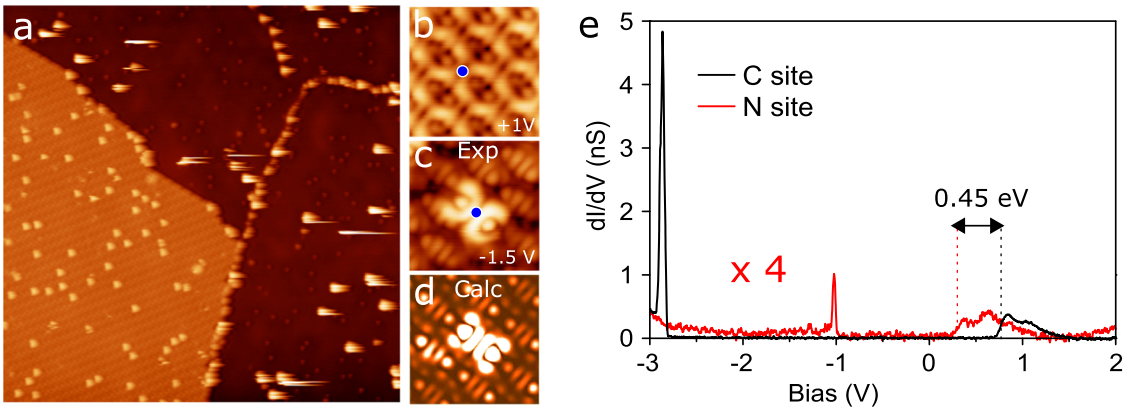

Fig. 4 TCNQ molecules on nitrogen doped graphene. **a** STM image of a TCNQ molecular island on nitrogen doped graphene (100×100 nm^2, $V = -1.5$ V, $I = 7$ pA). Experimental STM images at 1 V **b** and -1.5 V **c** (20 pA, 3×3 nm^2). **d** Calculated STM image under an electric field of 1.5 V/Å. **e** Representative d*I*/d*V* spectra recorded above molecules adsorbed on a C-site and a N-site. The blue dots in **b** and **c** mark the same position on the surface, and hence indicate the same molecule

reported for porphyrin on N-doped graphene.[16] Our ab initio calculations indicate that, for $\mathcal{E} = 0$, a TCNQ molecules at a N-site gains 0.33 *e*, as compared to 0.20 *e* at C-sites. Although our calculations show that the interaction of TCNQ with graphene is increased by the nitrogen doping, the binding of TCNQ on N-doped graphene is still of non-covalent nature (see supplementary information). As a consequence, the charging peak at a N-site shifts toward the Fermi level [see the red peak in Fig. 4e], since a lower electric field is required to bring the LUMO state to the Fermi level.

Further confirmation that the charging peak corresponds to the occupation of the LUMO state is provided by the experimental STM image at -1.5 V in Fig. 4c. We see that the bright molecule on the N-site has a significantly different shape (corresponding to the LUMO of TCNQ) from its neighbors on C-sites, since V_b^{ch} for molecules above nitrogen/carbon sites lies at a smaller/larger magnitude than -1.5 V. Thus, only the LUMO state of the molecule on a N-site becomes occupied. To confirm this interpretation, we obtain simulated STM images under the condition $\mathcal{E} = 1.5\,\mathrm{V/Å}$ and $V_b = 0.74$ V. Here, the LUMO for molecule on N- and C-sites is at 0.74 eV and 1.06 eV, respectively. Therefore, here one is mimicking the situation where one is at a bias voltage that includes the LUMO for a molecule above N, while remaining in the gap of the surrounding molecules. The resulting image [Fig. 4d] reproduces well the experimental image, confirming our interpretation.

In conclusion, we have shown that the tip-induced electric field shifts the molecular levels of TCNQ molecules on graphene, leading to a change of charge state at negative bias. Using ab initio calculations, we have shown that the molecule-on-graphene hybrid structure can be viewed as an electrostatic dipole with a dipole moment proportional to the electric field. As a consequence, the charge transfer, and therefore the electronic charge in the molecule and graphene, is tuned by the electric field. This allows one to charge the molecules by applying a large bias voltage in a STM experiment. The insertion of electron-donating point defects in graphene (nitrogen atoms) allows one to shift the energy levels of single molecules adsorbed directly above these N-sites. This allows one to selectively charge these molecules when the appropriate bias voltage is applied. As a consequence, in a compact 2D molecular island, it is possible to achieve a selective reduction of molecules adsorbed on N-sites. The field-dependent charge transfer is expected to arise whenever an electric field is present irrespective of whether it is applied by an STM tip or a backgate electrode. Our results therefore suggest that, under the application of a gate voltage and in the presence of defects, the electronic structure of molecules and graphene will undergo site-dependent shifts. This effect may be linked with the observation that defects in graphene play an important role in the sensitivity of chemical sensors.[31]

METHODS

Our STM experiments were performed under ultra-high vacuum conditions at 4.6 K, using a Scienta Omicron low temperature STM. d*I*/d*V* spectra were recorded through lock-in detection with a peak to peak modulation amplitude of 35 mV. Prior to the measurements on graphene, tungsten tips were calibrated on a Au(111) surface until the spectroscopy shows the Shockley state feature. Multilayer epitaxial graphene was grown on SiC $(000\bar{1})$ by annealing the SiC substrate in ultra high vacuum (UHV) at 1320 °C for 12 min under a silicon flux of ≈1 ML/min. Nitrogen doping was obtained by exposing the graphene sample to a flux of nitrogen radicals produced by a remote RF plasma source.[32] TCNQ molecules were deposited on samples held at 4.6 K using an effusion cell (Dr. Eberl MBE-Komponenten GmbH). The samples were then annealed to room temperature in order to obtain 2D islands, and subsequently reinserted in the STM stage.

Our DFT calculations were performed using the Quantum ESPRESSO package,[33] with a plane wave basis and ultrasoft pseudopotentials. Exchange-correlation interactions were treated within a generalized gradient approximation,[34] with van der Waals interactions incorporated using the DFT-D2 treatment.[35] An external electric field was applied via a sawtooth potential along the direction perpendicular to the plane of the TCNQ/graphene system.[36,37] The electronic charge was partitioned using the Bader prescription.[38] Simulated STM images were obtained using the Tersoff-Hamann approach.[39] The Kohn-Sham equations were expanded using plane wave basis set with kinetic energy and charge density cutoffs of 40 Ry and and 400 Ry, respectively.[40] The Brillouin zone was sampled using a $3 \times 3 \times 1$ k point mesh for the smallest possible unit cell of the TCNQ/graphene superstructure;[41] commensurate sampling was used for larger cells. Convergence has been improved by using Marzari-Vanderbilt smearing with a width of 0.001 Ry.[42] Interactions between periodic images were minimized by introducing a vacuum with a spacing of 14 Å along non-repeating directions. All the atomic coordinates were allowed to relax, until the Hellmann-Feynman forces on all atoms are less than 0.001 Ry/Bohr. For the TCNQ monolayer on nitrogen doped graphene the doping concentration was 0.22 %. The atomic structure of the TCNQ/graphene system used for calculations is displayed in supplementary information (Fig. S1).

DATA AVAILABILITY

The datasets generated during and/or analysed during the current study are available from the corresponding author on reasonable request.

ACKNOWLEDGEMENTS

The authors acknowledge support from CEFIPRA, the Indo-French Centre for the Promotion of Advanced Scienitific Research. ANR (Agence Nationale de la Recherche) and CGI/PIA (Commissariat Général à l'Investissement/Programme d'Investissement d'Avenir) ANR-11-IDEX-0005-02 are gratefully acknowledged for their financial support of this work through the Labex SEAM (Science and Engineering for Advanced Materials and devices) ANR 11 LABX 086. S.N. acknowledges support from the Sheikh Saqr Laboratory of ICMS, JNCASR.

AUTHOR CONTRIBUTIONS

V.D.P. and S.G. are co-first authors on this study. V.D.P., M.P.-F., and J.L. performed and analysed the STM experiments with support from C.C. V.R., Y.G., A.B., and S.R. S.G. and S.N. performed the ab initio calculations with support from Y.J.D. F.J. performed the synthesis of pristine and doped graphene under the supervision of R.S. V.D.P., S.G., S. N., and J.L. co-wrote the paper. All the authors discussed the results and commented on the manuscript.

ADDITIONAL INFORMATION

Supplementary information accompanies the paper on the *npj 2D Materials and Applications* website (https://doi.org/10.1038/s41699-019-0087-5).

Competing interests: The authors declare no competing interests.

Publisher's note: Springer Nature remains neutral with regard to jurisdictional claims in published maps and institutional affiliations.

REFERENCES

1. Hong, G. et al. Recent progress in organic molecule/graphene interfaces. *Nano Today* **8**, 388–402 (2013).
2. Wang, Q. H. & Hersam, M. C. Room-temperature molecular-resolution characterization of self-assembled organic monolayers on epitaxial graphene. *Nat. Chem.* **1**, 206–211 (2009).
3. Dong, X. et al. Doping single-layer graphene with aromatic molecules. *Small* **5**, 1422–1426 (2009).
4. Wang, X., Xu, J.-B., Xie, W. & Du, J. Quantitative analysis of graphene doping by organic molecular charge transfer. *J. Phys. Chem. C.* **115**, 7596–7602 (2011).
5. Cui, M. et al. Graphene-organic two-dimensional charge transfer complexes: inter-molecular electronic transitions and broadband near infrared photoresponse. *J. Phys. Chem. C* **122,** 7551-7556 (2018).
6. Coletti, C. et al. Charge neutrality and band-gap tuning of epitaxial graphene on SiC by molecular doping. *Phys. Rev. B* **81**, 235401 (2010).
7. Chen, W., Chen, S., Qi, D. C., Gao, X. Y. & Wee, A. T. S. Surface transfer p-type doping of epitaxial graphene. *J. Am. Chem. Soc.* **129**, 10418–10422 (2007).
8. Riss, A. et al. Imaging and tuning molecular levels at the surface of a gated graphene device. *ACS Nano* **8**, 5395–5401 (2014).
9. Wickenburg, S. et al. Tuning charge and correlation effects for a single molecule on a graphene device. *Nat. Commun.* **7**, 13553 (2016).
10. Lv, R. & Terrones, M. Towards new graphene materials: doped graphene sheets and nanoribbons. *Mater. Lett.* **78**, 209–218 (2012).
11. Wang, H., Maiyalagan, T. & Wang, X. Review on recent progress in nitrogen-doped graphene: synthesis, characterization, and its potential applications. *ACS Catal.* **2**, 781–794 (2012).
12. Wang, X. et al. Heteroatom-doped graphene materials: syntheses, properties and applications. *Chem. Soc. Rev.* **43**, 7067–7098 (2014).
13. Putri, L. K., Ong, W.-J., Chang, W. S. & Chai, S.-P. Heteroatom doped graphene in photocatalysis: a review. *Appl. Surf. Sci.* **358**, 2–14 (2015).
14. Wang, Y., Shao, Y., Matson, D. W., Li, J. & Lin, Y. Nitrogen-doped graphene and its application in electrochemical biosensing. *ACS Nano* **4**, 1790–1798 (2010).
15. Jeong, H. M. et al. Nitrogen-doped graphene for high-performance ultracapacitors and the importance of nitrogen-doped sites at basal planes. *Nano Lett.* **11**, 2472–2477 (2011).
16. Pham, V. D. et al. Electronic interaction between nitrogen-doped graphene and porphyrin molecules. *ACS Nano* **8**, 9403–9409 (2014).
17. Pham, V. D. et al. Molecular adsorbates as probes of the local properties of doped graphene. *Sci. Rep.* **6**, 24796 (2016).
18. de la Torre, B. et al. Non-covalent control of spin-state in metal-organic complex by positioning on N-doped graphene. *Nat. Commun.* **9**, 2831 (2018).
19. Torrente, I. F., Franke, K. J. & Pascual, J. I. Structure and electronic configuration of tetracyanoquinodimethane layers on a Au(1 1 1) surface. *Int. J. Mass Spectrom.* **277**, 269–273 (2008).
20. Barja, S. et al. Self-organization of electron acceptor molecules on graphene. *Chem. Commun.* **46**, 8198–8200 (2010).
21. Maccariello, D. et al. Spatially resolved, site-dependent charge transfer and induced magnetic moment in TCNQ adsorbed on graphene. *Chem. Mater.* **26**, 2883–2890 (2014).
22. Garnica, M. et al. Long-range magnetic order in a purely organic 2D layer adsorbed on epitaxial graphene. *Nat. Phys.* **9**, 368–374 (2013).
23. Fernández-Torrente, I., Kreikemeyer-Lorenzo, D., Stróżecka, A., Franke, K. J. & Pascual, J. I. Gating the charge state of single molecules by local electric fields. *Phys. Rev. Lett.* **108**, 036801 (2012).
24. Kocic, N. et al. Periodic charging of individual molecules coupled to the motion of an atomic force microscopy tip. *Nano Lett.* **15**, 4406–4411 (2015).
25. Pradhan, N. A., Liu, N., Silien, C. & Ho, W. Atomic scale conductance induced by single impurity charging. *Phys. Rev. Lett.* **94**, 076801 (2005).
26. Brar, V. W. et al. Gate-controlled ionization and screening of cobalt adatoms on a graphene surface. *Nat. Phys.* **7**, 43–47 (2011).
27. Wang, Y. et al. Mapping Dirac quasiparticles near a single Coulomb impurity on graphene. *Nat. Phys.* **8**, 653–657 (2012).
28. Teichmann, K. et al. Controlled charge switching on a single donor with a scanning tunneling microscope. *Phys. Rev. Lett.* **101**, 076103 (2008).
29. Metzger, R. M. MINDO/3-FP atom-in-molecule polarizabilities of TCNQ, TTF, TMPD, and of their radical ions. *J. Chem. Phys.* **74**, 3458–3471 (1981).
30. Metzger, R. M. Anisotropic semiconductors and metals: what holds them together? *Ann. NY Acad. Sci.* **313**, 145–165 (1978).
31. Kumar, B. et al. The role of external defects in chemical sensing of graphene field-effect transistors. *Nano Lett.* **13**, 1962–1968 (2013).
32. Joucken, F. et al. Localized state and charge transfer in nitrogen-doped graphene. *Phys. Rev. B* **85**, 161408 (2012).
33. Giannozzi, P. et al. QUANTUM ESPRESSO: a modular and open-source software project for quantum simulations of materials. *J. Phys. Condens. Matter* **21**, 395502 (2009).
34. Perdew, J. P., Burke, K. & Ernzerhof, M. Generalized gradient approximation made simple. *Phys. Rev. Lett.* **77**, 3865 (1996).
35. Grimme, S. Semiempirical GGA-type density functional constructed with a long-range dispersion correction. *J. Comput. Chem.* **27**, 1787–1799 (2006).
36. Kunc, K. & Resta, R. External fields in the self-consistent theory of electronic states: a new method for direct evaluation of macroscopic and microscopic dielectric response. *Phys. Rev. Lett.* **51**, 686 (1983).
37. Kozinsky, B. & Marzari, N. Static dielectric properties of carbon nanotubes from first principles. *Phys. Rev. Lett.* **96**, 166801 (2006).
38. Bader, R. F. W. *Atoms in molecules: a quantum theory*. (Oxford University Press, New York, 1990).
39. Tersoff, J. & Hamann, D. Theory and application for the scanning tunneling microscope. *Phys. Rev. Lett.* **50**, 1998 (1983).
40. Kohn, W. & Sham, L. J. Self-consistent equations including exchange and correlation effects. *Phys. Rev.* **140**, A1133–A1138 (1965).
41. Monkhorst, H. J. & Pack, J. D. Special points for Brillouin-zone integrations. *Phys. Rev. B* **13**, 5188 (1976).
42. Marzari, N., Vanderbilt, D., De Vita, A. & Payne, M. C. Thermal contraction and disordering of the Al(110) surface. *Phys. Rev. Lett.* **82**, 3296–3299 (1999).